

**DETERMINATION OF THE POST-CRITICAL STATE OF
COMPRESSED PLATES WITHIN THE BI-NONLINEAR
THEORY**

FRANCISZEK ROMANÓW
PRZEMYSŁAW NAJDYCHOR

Institute of Mechanics and Machinery Construction Fundamentals, University of Zielona Góra
e-mail: F.Romanow@ibmp.uz.zgora.pl; P.Najdychor@ibmp.uz.zgora.pl

In a majority of strength problems related to sandwich structures the concept of the linear displacement state is used. This state of displacements is defined with the help of the broken line hypothesis, which is used for the determination of critical states within the geometrically linear theory and for analysis of post-critical states of geometrically non-linear theory.

In the paper, taking into account the non-linear displacement state of the core and the geometrically linear theory for faces and core (binonlinear theory), we carry out an analysis of post-critical loads. The problem is solved by means of the energy method. The post-critical stresses are described by a general formula applied also for a uni-axial compressed plate simply supported at both edges.

Key words: sandwich plates, the bi-nonlinear theory, post-critical

1. Introduction

The strength and stability of sandwich structures with a soft foam core is usually analysed by means of the linear displacement state of the core and faces (linear hypothesis) (Grądzki and Kowal-Michalska, 2000; Hop, 1980; Magnucki and Oswald, 2001; Planterma, 1966; Stam and Witte, 1973; Szyc, 1971; Twardosz and Hong-Thai, 1975). The above assumption confines calculation methods to thin wall structures.

A survey of Polish scientific results related to the calculation and investigation of sandwich structures on the turn of the 20th century has been presented in Romanów (2001), Biliński and Kmita (2000).

Non-linear analysis of stability of sandwich structures based upon the linear hypothesis of the displacement state was already published in the seventies of the last century, (e.g. Szyc, 1971; Twardosz and Hong-Thai, 1975).

With the help of the idea of the linear displacement state, for the core and faces, papers taking into account the post-elastic state have also been presented (e.g. Grądzki and Kowal-Michalska, 2000; Zielnica, 1981).

In a paper by Grądzki and Kowal-Michalska (2000) post-critical states in the elastoplasticity range were analysed. An example of a compressed three layer plate (steel-aluminium-steel) was given. In all the authors' papers, in contrast to others, the non-linear core displacement state hypothesis was used. By analogy with the linear hypothesis, this state can be shortly denoted as the hyperbolic hypothesis.

A comprehensive set of knowledge and varied applications of the hyperbolic hypothesis can be found in Romanów (1995).

In the present paper, the post-critical loads for the three-layer plate are presented. The faces are made of steel, the core is made of foam. The plate is compressed in one direction with a unit force N_x which is uniformly distributed along simply supported edges (for $x = 0; x = a$). The other two sides of the plate are free. An example of a plate is given in Fig. 1.

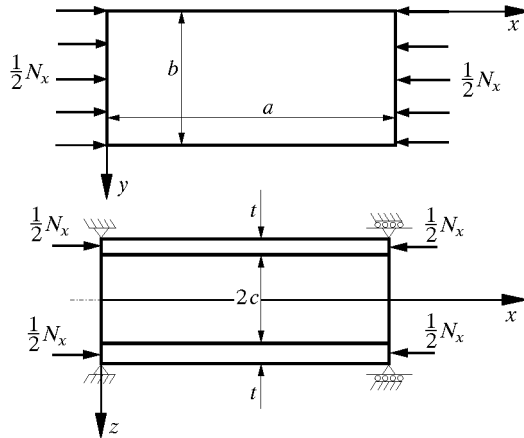


Fig. 1. A compressed sandwich plate and compressive load

The problem is characterized by the core non-linear displacement state and takes into account the geometrically non-linear theory for the faces and core. So, such an approach can be named a bi-nonlinear theory.

A similar analysis was presented in Romanów *et al.* (2001). There, the post-critical states for a compressed homogeneous plate fastened with two external

layers, were analysed. Here, kinematic functions are given at two parallel edges. By using a simplified function $\phi(z)$ transversal non-linear displacements for core are taken into account.

2. Displacement and strain state

The displacements U and W of the faces in the x and y directions must satisfy boundary conditions for the thus supported plate

$$U_i = B_m \cos \beta x \quad W_i = A_m \sin \beta x \quad \beta = \frac{m\pi}{a} \quad (2.1)$$

where m is the number of half-waves of the displacement state of faces of a unilaterally compressed plate after stability loss ($m = 1, 2, 3, \dots$). These expressions describe mid-face plane displacements. Hence, the mid point displacement O is equal to $U^+ = (U_1 + U_2)/2$ and related to rotation $U^- = (U_1 - U_2)/2$. The complete face displacement state is described by a linear function of the variable z

$$U = U_i - \left(z \pm c \pm \frac{t}{2} \right) \frac{\partial W_i}{\partial x} \quad (2.2)$$

The superscript "+" refers to faces in the interval $-c - t \leq z \leq c$, the lower one "-" refers to $c \leq z \leq c + t$.

The core displacement state of considered plate (biaxial displacement state) is described by formulas (Appendix 1)

$$U_r = U^+ - \frac{z}{c} \left(U^- - \frac{t}{2} \frac{\partial W}{\partial x} \right) F(z) \quad W_r = WT(z) \quad (2.3)$$

which Result from (A8)₂, where $V_r = 0$.

The functions F and T depend on the variable z only, and are expressed by hyperbolic functions (formulas (A6), (A7) in Appendix 1). The constants H_i appearing in these formulas are discussed in Appendix 2. When the functions $F(z)$ and $T(z)$ are equal to one, then formulas (2.3) describe the linear displacement state (broken line hypothesis).

The face and core strains are non-linear relations, and are defined by formulas

$$\begin{aligned} \varepsilon_x &= \frac{\partial U}{\partial x} + \frac{1}{2} \frac{\partial W^2}{\partial x} & \varepsilon_{xr} &= \frac{\partial U_r}{\partial x} + \frac{1}{2} \frac{\partial W_r^2}{\partial x} \\ \varepsilon_{zr} &= \frac{\partial W_r}{\partial z} + \frac{1}{2} \left(\frac{\partial W_r}{\partial z} \right)^2 & \gamma_{xsr} &= \frac{\partial U_r}{\partial z} + \frac{\partial W_r}{\partial x} + \frac{\partial W_r}{\partial z} \frac{\partial W_r}{\partial x} \end{aligned} \quad (2.4)$$

3. Elastic energy of the plate

The total energy of the plate is composed of two terms: the first term corresponds to the core energy E_r , the second one to the energy of faces E_o

$$E_c = E_r + E_o \quad (3.1)$$

$$E_r = G_r \int_0^a \int_{-c}^c \left[\left(1 + \frac{\nu_r}{1 - 2\nu_r} \right) (\varepsilon_{xr}^2 + \varepsilon_{zr}^2) + \frac{2\nu_r}{1 - 2\nu_r} \varepsilon_{xr} \varepsilon_{zr} + \frac{1}{2} \gamma_{xsr} \right] dx dz$$

where G and ν are Kirchoff's modulus and Poisson's ratio, respectively.

Taking into account (2.3) and (2.4), one can get a formula for the core energy expressed by the displacements U and W

$$\begin{aligned} E_r = & G_r d_1 \int_0^a \left(\frac{1}{c^2} \frac{\partial U^2}{\partial x} F_1 - \frac{t}{c^2} \frac{\partial U}{\partial x} \frac{\partial^2 W}{\partial x^2} F_1 + \frac{t^2}{4c^2} \frac{\partial^2 W}{\partial x^2} F_1 + W^2 F_5 + \right. \\ & \left. + \frac{1}{4} \frac{\partial W^4}{\partial x} F_{16} + \frac{W^4}{4} F_{19} \right) dx + \\ & + G_r d_2 \int_0^a \left(-\frac{2W}{c} \frac{\partial U}{\partial x} F_9 + \frac{tW}{c} \frac{\partial^2 W}{\partial x^2} F_9 + \frac{W^2}{2} \frac{\partial W^2}{\partial x} F_{22} \right) dx + \quad (3.2) \\ & + G_r \int_0^a \left(\frac{U^2}{2c^2} F_{10} - \frac{tU}{2c^2} \frac{\partial W}{\partial x} F_{10} + \frac{t^2}{8c^2} \frac{\partial W^2}{\partial x} F_{10} + \frac{1}{2} \frac{\partial W^2}{\partial x} F_{11} - \frac{U}{c} \frac{\partial W}{\partial x} F_{12} \right) dx + \\ & + G_r \int_0^a \left(\frac{t}{2c} \frac{\partial W^2}{\partial x} F_{12} + \frac{1}{2} W^2 \frac{\partial W^2}{\partial x} F_{22} \right) dx \end{aligned}$$

where F_1 - F_{22} are certain integrals of hyperbolic functions, see Appendix 2, but the expressions described in italics contain non-linear elements.

The elastic energy of the faces is described by means of the formula

$$E_o = B^* \int_0^a \frac{\partial U}{\partial x} dx + D \int_0^a \frac{\partial^2 W^2}{\partial x^2} dx + \frac{1}{4} B^* \int_0^a \frac{\partial W^4}{\partial x} dx \quad (3.3)$$

where E^* – Young's modulus, t – face thickness, a – plate length, b – its width and

$$B^* = \frac{E^* t}{1 - \nu^2} \quad D = \frac{E^* t^3}{12(1 - \nu^2)}$$

The work of external forces is described by

$$L_z = -\frac{1}{2} \int_0^a N_x \frac{\partial W^2}{\partial x} dx \quad (3.4)$$

The potential energy of the whole plate is given by the sum of (3.2), (3.3) and (3.4)

$$P = E_o + E_r + L_z \quad (3.5)$$

From the minimum condition of the potential, two equations are obtained

$$\frac{\partial P}{\partial A_m} = 0 \quad \frac{\partial P}{\partial B_m} = 0 \quad (3.6)$$

resulting in an expression for the loading N_x

$$N_x = \frac{A_m^2 R_6 + (R_1 - R_1 R_5)}{R_4} \quad (3.7)$$

Formula (3.7) can be transformed into

$$\alpha = \frac{N_x}{N_{xkr}} = \frac{A_m^2 R_7}{N_{xkr}} + 1 \quad (3.8)$$

The last expression defines a relation between the post-critical loads N_x and deflection amplitude of the face A_m . This is a quadratic equation for the independent variable A_m . If $A_m = 0$, then eqyation (3.8) can be used to obtain the critical load of the plate

$$N_{xkr} = \frac{R_1 - R_1 R_5}{R_4} \quad (3.9)$$

where

$$\begin{aligned} R_1 &= A_m^2 G_r \left[\beta^2 \frac{at}{c} \left(F_1 d_1 \beta^2 \frac{t}{4c} - F_9 d_2 + F_{10} \frac{t}{8c} + \frac{1}{2} F_{12} \right) + \beta^2 F_{11} \frac{a}{2} \right] + A_m^2 D \beta^4 a \\ R_2 &= A_m B_m \left[G_r \beta \left(d_2 F_9 \frac{a}{c} - \frac{at}{2c^2} d_1 F_1 \beta^2 - \frac{at}{4c^2} F_{10} - \frac{a}{2c} F_{12} \right) \right] \\ R_3 &= B_m^2 \left[G_r \left(F_1 d_1 \beta^2 \frac{a}{2c^2} + F_{10} \frac{a}{4c^2} \right) + B^* \beta^2 \frac{a}{2} \right] \\ R_4 &= \frac{ab}{2} \beta^2 \quad R_5 = \frac{R_1}{R_3} \quad R_7 = \frac{R_6}{R_4} \\ R_6 &= A_m^4 \left[G_r \left(d_1 F_{16} \beta^4 \frac{3a}{8} + d_1 F_{19} \frac{3a}{8} + F_{22} \beta^2 \frac{a}{4} + d_2 F_{22} \beta^2 \frac{a}{4} \right) + B^* \beta^4 \frac{3a}{8} \right] \end{aligned}$$

3.1. Examples

For given values of the plate parameters

$$\begin{aligned} a &= 0.285 \text{ m} & b &= 0.185 \text{ m} & \nu_r &= 0.17 \\ \nu &= 0.3 & E_r^* &= 58.9 \cdot 10^6 \text{ Pa} & E^* &= 68694.8 \cdot 10^6 \text{ Pa} \\ t &= 0.001 \text{ m} \end{aligned}$$

the following results have been obtained, see (3.9).

Table 1. Critical loads versus core thickness

c [m]	N_{xkr} [N/m]	m
0.004	28961	1
0.005	36034	1
0.008	60040	1
0.010	77525	1
0.0176	99271	11
0.0185	99350	11
0.020	142754	13
0.050	143383	13

For these data, the dependence of the critical force, (see (3.9), on the core thickness is presented in Table 1. A similar relation is presented in Fig. 2.

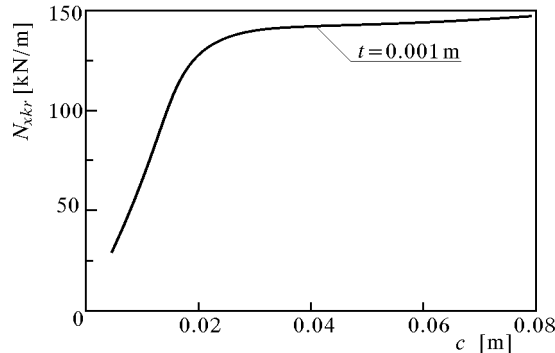


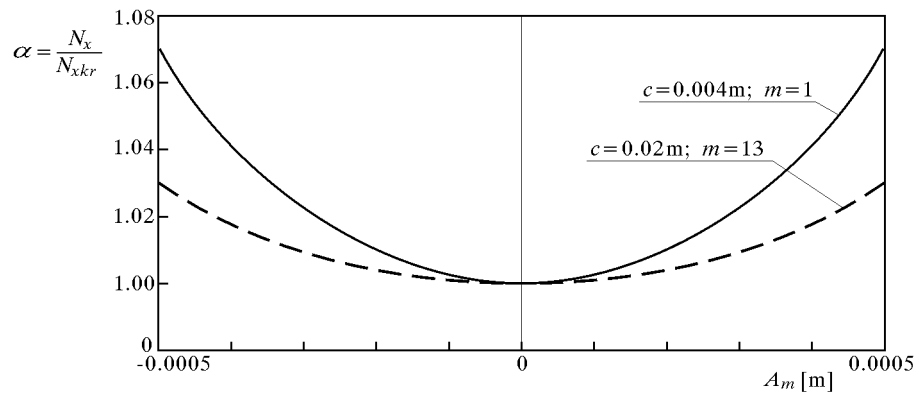
Fig. 2. The critical force N_{xkr} versus core thickness

A dependence of the coefficient α on the amplitude A_m , Eq. (3.8), where $m = 1$ (thin plates) and $m = 13$ (thick plates), is presented in Table 2.

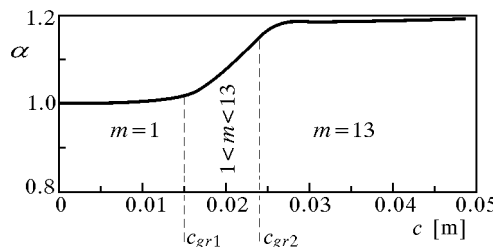
The criteria for the division into thin, medium and thick sandwich plates are described by Romanów (1995).

Table 2. Dependence of the coefficient α on the amplitude A_m , Eq. (3.8)

$c = 0.004 \text{ m}; m = 1$						
A_m	+0.0005	+0.0004	+0.0003	+0.0002	+0.0001	0
α	1.07	1.04	1.024	1.01	1.003	1
$c = 0.02 \text{ m}; m = 13$						
A_m	+0.0005	+0.0004	+0.0003	+0.0002	+0.0001	0
α	1.009	1.0063	1.0035	1.0016	1.0004	1

Fig. 3. Dependence of the coefficient α on the amplitude A_m

In Fig. 4 the dependence of the coefficient α on the core thickness c is presented.

Fig. 4. Influence of the core thickness on the coefficient α

It is seen in the diagram that the whole region of the core thickness can be divided into three sub-regions:

- In the first sub-region $0 \leq c \leq c_{gr1} = 0.017$, α increases with the core thickness, but does not significantly differ from the unit. The plates

belonging to that region are called thin plates and the number of half-waves m is equal to one. In that region, the broken line hypothesis and hyperbolic hypothesis give similar results.

- In the second sub-region the number of half waves depends on the core thickness. It corresponds to $c_{gr1} \leq c \leq c_{gr2} = 0.0235$, $1 < m < 13$. These are medium thickness plates.
- The third sub-region is defined by the core thickness $c \geq c_{gr2}$. In this zone, the half-wave number m has a constant value ($m = 13$) and the coefficient α is slowly changing with increase in the core thickness and tends asymptotically to a constant value. From that it can be seen that assumption of $c > c_{gr2}$ is uneconomical, because the plate weight increases, while α is practically constant.

With the help of formulas (3.9) and (3.7), one can calculate the resultant force acting upon the plate

$$N_{kr} = N_{xkr}b \quad N_{xn} = N_x b \quad (3.10)$$

or related stresses

$$\sigma_{kr} = \frac{N_{xkr}}{2t} \quad \sigma_{xn} = \frac{N_x}{2t} \quad (3.11)$$

A. Appendix 1

Up to the present, methods of calculation of sandwich structures have taken into account linear displacement states of faces and core. This is the so-called broken line hypothesis. In Fig. 5, the displacements in the x -axis direction are presented by means of segments AC^- , CE^- (broken line) and EG^- . This means that only displacements in the x -direction and constant displacements of the three layers in the vertical direction are taken into account for the faces and core.

In the x -direction, the core displacement is described by a linear function in z

$$U_r^* = U^+ - \frac{z}{c} \left(U^- - \frac{t}{2} \frac{\partial W}{\partial x} \right) \quad (A.1)$$

but in the direction vertical with respect to the plate surface, the core displacement (deflection) is constant along the whole thickness

$$W_r^* = W \quad (A.2)$$

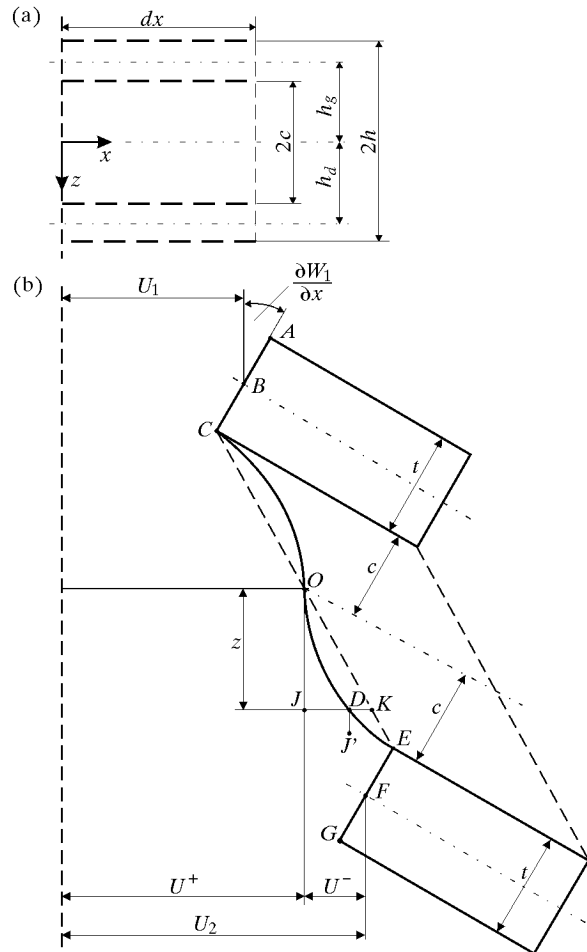


Fig. 5. Longitudinal displacement of the core (illustration of the hyperbolic hypothesis) (a) before strain, (b) after strain

It is assumed that the core in the vertical direction cannot be strained. This means that it is infinitely rigid ($E_r^* = \infty$). The geometrical meaning of this is as follows: a random point J (Fig. 5), located upon a cross-section of the core, is displaced parallel to the x -axis up to the point K . The geometrical set of points K forms the segment \overline{COKE} . For real core parameters ($E_r^* \neq \infty$), J is displaced into point J' , and its projection upon the x -axis is denoted by D .

From geometrical relations, the formula

$$JK^- = \frac{z}{c} \left(-U^- + \frac{t}{2} \frac{\partial W}{\partial x} \right) \quad (\text{A.3})$$

is obtained. A variable segment JD^- can be defined by the function

$$JD^- = JK^- F(z) = -\frac{z}{c} \left(U^- - \frac{t}{2} \frac{\partial W}{\partial x} \right) F(z) \quad (\text{A.4})$$

The total displacement of the point D in the x -direction will be equal to the sum of the average displacement U^+ of the point O and the segment JD^- . In other words

$$U_r = U^+ - \frac{z}{c} \left(U^- - \frac{t}{2} \frac{\partial W}{\partial x} \right) F(z) \quad (\text{A.5})$$

The set of points D related to the core thickness forms the curve EDOC, the shape of which depends on the function $F(z)$. In the general case, taking into account the tri-axial core displacement state, from the three equilibrium equations for the core element and from the boundary conditions $z = 0, z = c, \partial F(0)/\partial x = 0$ and $F(c) = 1$, one can get the hyperbolic function

$$F(z) = H_1 \cosh \lambda z + H_2 \frac{\sinh \lambda z}{z} \quad (\text{A.6})$$

In the same way, in the plane yz , one can get

$$S(z) = H_3 \cosh \lambda z + H_4 \frac{\sinh z}{z} \quad (\text{A.7})$$

and in the direction perpendicular to the plate plane

$$T(z) = H_5 \cosh \lambda z + H_6 z \sinh \lambda z \quad (\text{A.8})$$

$$\lambda = \sqrt{\beta^2 + \rho^2} = \sqrt{\left(\frac{\Pi m}{a}\right)^2 + \left(\frac{\Pi n}{b}\right)^2} \quad (\text{A.9})$$

Ultimately, displacements of a random point J in the x, y, z directions are defined by the functions

$$\begin{aligned} U_r &= U^+ - \frac{z}{c} \left(U^- - \frac{t}{2} \frac{\partial W}{\partial x} \right) F(z) \\ V_r &= V^+ - \frac{z}{c} \left(V^- - \frac{t}{2} \frac{\partial W}{\partial y} \right) S(z) \\ W_r &= WT(z) \end{aligned} \quad (\text{A.10})$$

B. Appendix 2

$$\begin{aligned}
H_1 &= -C_2 \frac{c}{r} & H_2 &= \left(1 + C_2 \frac{c}{r} \cosh \lambda c\right) \\
H_4 &= (1 - H_3 \cosh \lambda c) \frac{c}{\sinh \lambda c} & H_3 &= -C_2 \frac{\rho c}{\beta p_1} \\
H_5 &= \left(1 - C_2 \frac{c\lambda}{\beta} \sinh \lambda c\right) \frac{1}{\cosh \lambda c} & H_6 &= \frac{\lambda}{\beta} C_2 \\
C_2 &= -\frac{\beta C [\lambda \sinh \lambda c + (\beta r + \rho p_1) \cosh \lambda c]}{\lambda (2 + C) \sinh \lambda c \cosh \lambda c + \lambda^2 c C} & r &= \frac{B_{mn}}{A_{mn}} - \frac{t\beta}{2} \\
p_1 &= \frac{C_{mn}}{A_{mn}} - \frac{t\rho}{2} & C &= \frac{1}{(1 - 2\nu_r)}
\end{aligned}$$

For the given task the value amount $\lambda = \beta$, $V_r = 0$

$$\begin{aligned}
F_1 &= H_1^2 X_1 + 2H_1 H_2 X_2 + H_2^2 X_3 \\
F_5 &= (H_5^2 \beta^2 + H_6^2 + 2H_5 H_6 \beta) X_3 + (2H_5 H_6 \beta^2 + 2H_6^2 \beta) X_2 + H_6^2 \beta^2 X_1 \\
F_9 &= (H_1 H_5 \beta + H_1 H_6 + H_2 H_6 \beta) X_2 + (H_2 H_5 \beta + H_2 H_6) X_3 + H_1 H_6 \beta X_1 \\
F_{10} &= (H_1^2 + H_2^2 \beta^2 + 2H_1 H_2 \beta) X_5 + (2H_1^2 \beta + 2H_1 H_2 \beta^2) X_2 + H_1^2 \beta^2 X_4 \\
F_{11} &= H_5^2 X_5 + 2H_5 H_6 X_2 + H_6^2 X_4 \\
F_{12} &= (H_1 H_5 + H_2 H_5 \beta) X_5 + (H_1 H_6 + H_1 H_5 \beta + H_2 H_6 \beta) X_2 + H_1 H_6 \beta X_4 \\
F_{16} &= H_5^4 X_6 + 4H_5^3 H_6 X_7 + 6H_5^2 H_6^2 X_8 + 4H_5 H_6^3 X_9 + H_6^4 X_{10} \\
F_{19} &= (H_5^4 \beta^4 + H_6^4 + 4H_5^3 H_6 \beta^3 + 6H_5^2 H_6^2 \beta^2 + 4H_5 H_6^2 \beta) X_{11} + \\
&\quad + (4H_5^3 H_6 \beta^4 + 12H_5^2 H_6^2 \beta^3 + 12H_5 H_6^3 \beta^2 + 4H_6^4 \beta) X_{12} + \\
&\quad + (6H_5^2 H_6^2 \beta^4 + 12H_5 H_6^3 \beta^3 + 6H_6^4 \beta^2) X_8 + \\
&\quad + (4H_5 H_6^3 \beta^4 + 4H_6^4 \beta^3) X_{13} + H_6^4 \beta^4 X_{14} \\
F_{22} &= (H_5^4 \beta^2 + 2H_5^3 H_6 \beta + H_5^2 H_6^2) X_{15} + (2H_5^3 H_6 \beta^2 + 2H_5^2 H_6^2 \beta) X_7 + \\
&\quad + H_5^2 H_6^2 \beta^2 X_{16} + (2H_5^3 H_6 \beta^2 + 4H_5^2 H_6^2 \beta + 2H_5 H_6^3) X_{12} + \\
&\quad + (4H_5^2 H_6^2 \beta^2 + 4H_5 H_6^3 \beta) X_8 + 2H_5 H_6^3 \beta^2 X_{13} + \\
&\quad + (H_5^2 H_6^2 \beta^2 + 2H_5 H_6^3 \beta + H_6^4) X_{17} + (2H_5 H_6^3 \beta^2 + 2H_6^4 \beta) X_{19} + H_6^4 \beta^2 X_{18}
\end{aligned}$$

$$\begin{aligned}
X_1 &= \int_{-c}^c z^2 \cosh^2 \beta z \, dz & X_2 &= \int_{-c}^c z \sinh \beta z \cosh \beta z \, dz \\
X_3 &= \int_{-c}^c \sinh^2 \beta z \, dz & X_4 &= \int_{-c}^c z^2 \sinh^2 \beta z \, dz
\end{aligned}$$

$$\begin{aligned}
 X_5 &= \int_{-\frac{c}{\beta}}^{\frac{c}{\beta}} \cosh^2 \beta z \, dz & X_6 &= \int_{-\frac{c}{\beta}}^{\frac{c}{\beta}} \cosh^4 \beta z \, dz \\
 X_7 &= \int_{-\frac{c}{\beta}}^{\frac{c}{\beta}} z \sinh \beta z \cosh^3 \beta z \, dz & X_8 &= \int_{-\frac{c}{\beta}}^{\frac{c}{\beta}} z^2 \sinh^2 \beta z \cosh^2 \beta z \, dz \\
 X_9 &= \int_{-\frac{c}{\beta}}^{\frac{c}{\beta}} z^3 \sinh^3 \beta z \cosh \beta z \, dz & X_{10} &= \int_{-\frac{c}{\beta}}^{\frac{c}{\beta}} z^4 \sinh^4 \beta z \, dz \\
 X_{11} &= \int_{-\frac{c}{\beta}}^{\frac{c}{\beta}} \sinh^4 \beta z \, dz & X_{12} &= \int_{-\frac{c}{\beta}}^{\frac{c}{\beta}} z \sinh^3 \beta z \cosh \beta z \, dz \\
 X_{13} &= \int_{-\frac{c}{\beta}}^{\frac{c}{\beta}} z^3 \sinh \beta z \cosh^3 \beta z \, dz & X_{14} &= \int_{-\frac{c}{\beta}}^{\frac{c}{\beta}} z^4 \cosh^4 \beta z \, dz \\
 X_{15} &= \int_{-\frac{c}{\beta}}^{\frac{c}{\beta}} \sinh^2 \beta z \cosh^2 \beta z \, dz & X_{16} &= \int_{-\frac{c}{\beta}}^{\frac{c}{\beta}} z^2 \cosh^4 \beta z \, dz \\
 X_{17} &= \int_{-c}^{c} z^2 \sinh^4 \beta z \, dz & X_{18} &= \int_{-c}^{c} z^4 \sinh^2 \beta z \cosh^2 \beta z \, dz
 \end{aligned}$$

References

1. BILIŃSKI T., KMITA J., 2000, *Dorobek nauki polskiej w zakresie konstrukcji zespolonych*, Wydawnictwo Zachodnie Centrum Organizacji, Politechnika Zielonogórska
2. GRĄDZKI R., KOWAL-MICHALSKA K., 2000, Nośność ściskanych wielowarstwowych płyt prostokątnych, *IX Sympozjon Stateczności Konstrukcji*, Zakopane, 53-60
3. HOP T., 1980, *Konstrukcje warstwowe*, Arkady Warszawa
4. MAGNUCKI K., OSWALD M., 2001, *Stateczność i optymalizacja konstrukcji warstwowych*, Poznań-Zielona Góra
5. PLANTERMA F.J., 1966, *Sandwich Construction*, John Wiley-Sonc, Inc. New York
6. ROMANÓW F., 1995, *Wytrzymałość konstrukcji warstwowych*, WSI Zielona Góra
7. ROMANÓW F., 2001, *Wkład polskich uczonych w rozwój metod obliczeniowych i badań konstrukcji warstwowych*, *Polska Mechanika u progu XXI wieku*, Oficyna Wydawnicza Politechniki Warszawskiej. Kazimierz Dolny-Warszawa, 123-134

8. ROMANÓW F., NAJDYCHOR P., BEJENKA S., 2001, Stany nadkrytyczne ścisanych jednorodnych płyt usztywnionych zewnętrznymi warstwami, *II Symposjon Kompozyty-Konstrukcje Warstwowe*, PTMTS oddział we Wrocławiu,, Wrocław-Karpacz, 199-204
9. STAM K., WITTE H., 1973, *Sandwichkonstruktionen*, Springer-Verlag, Wien, New York
10. SZYC W., 1971, Nieliniowe zagadnienia stateczności sprężystej, trójwarstwowej otwartej powłoki walcowej, *Rozprawy inżynierskie*, **19**
11. TWARDOSZ F., HONG-THAI D., 1975, Stateczność trójwarstwowej otwartej powłoki walcowej poddanej ścinaniu, *Archiwum Budowy Maszyn*, **3**
12. ZIELNICA J., 1981, Wyboczenie trójwarstwowej powłoki stożkowej poza zakresem sprężystym przy obciążeniu złożonym, *Rozprawy inżynierskie*, 453-470

Określenie stanu naprężeń nadkrytycznych ścisanych płyt warstwowych z uwzględnieniem teorii binieliniowej

Streszczenie

Większość problemów wytrzymałościowych dotyczących konstrukcji warstwowych analizowana jest na podstawie liniowego stanu przemieszczeń. Ten stan przemieszczeń zdefiniowano za pomocą hipotezy linii łamanej. Hipoteza wykorzystywana jest zarówno do określenia stanów krytycznych w ujęciu geometrycznie liniowej teorii, jak i w ujęciu geometrycznie nieliniowej teorii – do analizy stanów nadkrytycznych.

W niniejszej pracy przedstawiono analizę nadkrytycznych obciążzeń z uwzględnieniem nieliniowego stanu przemieszczeń rdzenia oraz geometrycznie nieliniowej teorii dla okładzin i rdzenia (binieliniowa teoria).

Problem rozwiązyano przy pomocy metody energetycznej, a nadkrytyczne naprężenia opisano ogólnym wzorem, na podstawie którego przeanalizowano przykład jednoosiowo ścisanej płyty przegubowo podpartej na dwóch krawędziach.

Manuscript received January 12, 2004; accepted for print March 30, 2004